

# Intrinsic and Task-Evoked Network Architectures of the Human Brain

Michael W. Cole,<sup>1,2,\*</sup> Danielle S. Bassett,<sup>3</sup> Jonathan D. Power,<sup>4</sup> Todd S. Braver,<sup>2</sup> and Steven E. Petersen<sup>2,4</sup>

<sup>1</sup>Center for Molecular and Behavioral Neuroscience, Rutgers University, Newark, NJ 07102, USA

<sup>2</sup>Department of Psychology, Washington University, St. Louis, MO 63130, USA

<sup>3</sup>Department of Bioengineering, University of Pennsylvania, Philadelphia, PA 19104, USA

<sup>4</sup>Department of Neurology, Washington University, St. Louis, MO 63110, USA

\*Correspondence: michael.cole@rutgers.edu

<http://dx.doi.org/10.1016/j.neuron.2014.05.014>

## SUMMARY

Many functional network properties of the human brain have been identified during rest and task states, yet it remains unclear how the two relate. We identified a whole-brain network architecture present across dozens of task states that was highly similar to the resting-state network architecture. The most frequent functional connectivity strengths across tasks closely matched the strengths observed at rest, suggesting this is an “intrinsic,” standard architecture of functional brain organization. Furthermore, a set of small but consistent changes common across tasks suggests the existence of a task-general network architecture distinguishing task states from rest. These results indicate the brain’s functional network architecture during task performance is shaped primarily by an intrinsic network architecture that is also present during rest, and secondarily by evoked task-general and task-specific network changes. This establishes a strong relationship between resting-state functional connectivity and task-evoked functional connectivity—areas of neuroscientific inquiry typically considered separately.

## INTRODUCTION

Recent advances in human neuroimaging have led to numerous studies characterizing interregional temporal relationships during task and resting states (Fox and Greicius, 2010; Friston, 2011). Initial functional connectivity (FC) studies focused on FC during task states (Friston, 1994), yet FC during the resting state has come to dominate the field (Biswal et al., 2010). There are many reasons for this shift in focus, although perhaps the most influential is the notion that resting-state FC may characterize an “intrinsic” functional network architecture that is present across many (or all) brain states (Fox and Raichle, 2007; Vincent et al., 2007), much like structural connectivity. If true, this would greatly simplify the study of functional brain organization—from needing to consider a virtually infinite variety of task states to

considering a state space strongly constrained by a single (or few) network architecture(s). Thus, determining the universality of the resting-state network architecture is an important step toward understanding the brain’s functional organization.

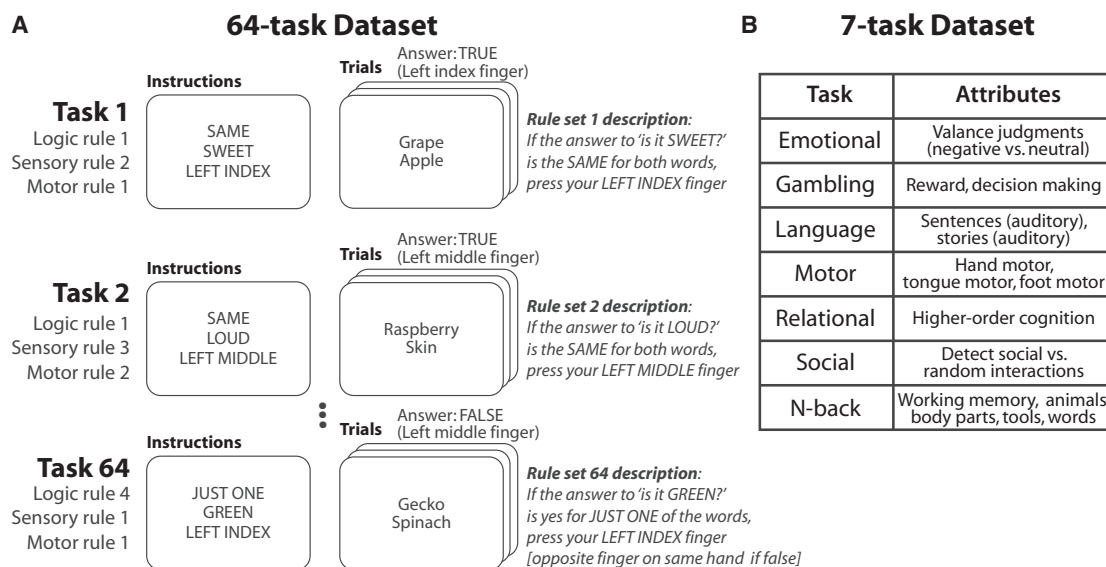
Most comparisons between task and rest FC have observed high correspondence (Fair et al., 2007; Fox et al., 2007; Greicius et al., 2003), but these comparisons have been limited to small sets of task states and connections. More recent comparisons between task and rest FC have emphasized differences in FC patterns, also during a small number of task states (Buckner et al., 2013; Hermundstad et al., 2013; Mennes et al., 2013). Thus, some studies advocate a more universal architecture, while others advocate differential task and resting architectures.

We sought to test for universality of the resting-state network architecture in a more comprehensive manner by using large-scale graphs built from FC among hundreds of brain regions encompassing every major brain system (Power et al., 2011) across dozens of task states (Barch et al., 2013; Cole et al., 2010) and rest. We hypothesized that resting-state FC would reveal an intrinsic network architecture that would also be present across a wide variety of task states. We also hypothesized that some task-evoked FC changes from this intrinsic architecture would be evident (“evoked” network architectures) but that these evoked changes would tend to be small and be restricted to a relatively small number of connections for any given task. This would suggest that the intrinsic network architecture represents a standard state of brain organization that is modified as necessary to implement task demands. Generally, this would help bridge resting-state FC and task FC findings in the literature, facilitating a more comprehensive account of human brain organization.

## RESULTS

### Detecting the Human Brain’s Intrinsic and Evoked Network Architectures

It may be that evoked FC changes occur in the presence of an intrinsic functional network architecture that extends across many or all brain states (e.g., rest and tasks). To address this question, we used fMRI to measure temporal relationships between hundreds of brain regions across dozens of task states and rest in single subjects. Two data sets were used. The first data set involved the permuted rule operations cognitive paradigm (Cole et al., 2010) that contained 12 rules that were

**Figure 1. Testing Multiple Tasks per Subject**

(A) The first fMRI data set involved 64 distinct tasks, composed of unique combinations of task rules (Cole et al., 2010). Each subject ( $n = 15$ ) performed all 64 tasks.

(B) The second data set involved seven tasks chosen to elicit the involvement of all major cognitive domains and brain systems (Barch et al., 2013). Each subject ( $n = 118$ ) performed all seven tasks.

permuted into 64 distinct task states in short task blocks (Figure 1A). Tasks were defined as distinct cognitive processes, such that the same stimuli could be presented across each of the 64 tasks, but distinct cognitive processes would be necessary to respond correctly to each one. Importantly, this paradigm isolated cognitive task set differences by minimizing perceptual changes across tasks (e.g., changes in visual field, sensory modality). To extend and test the robustness of findings from the 64-task data set, we also conducted analyses with a Human Connectome Project data set (118 subjects) that included rest and a set of seven tasks (Figure 1B) (Barch et al., 2013). The seven tasks were highly distinct from one another, although they also differed in basic perceptual aspects (e.g., changes in visual field, sensory modality), which could be a larger driver of FC differences than cognitive task set differences. FC was estimated as temporal correlations (Zalesky et al., 2012) among a set of 264 putative functional regions throughout the brain (defined independently to reduce potential statistical biases) (Power et al., 2011). These correlations were estimated for task FC after regressing out (across-trial mean) task-evoked activations and removing the short rest periods between task blocks from each region's time series.

In addition to testing for the existence of an intrinsic network architecture—an architecture common across rest and multiple task states—we sought to identify interregional connections unique to each task state, together comprising a set of evoked network architectures. To estimate both intrinsic and evoked architectures simultaneously, we used a tool (multislice community detection) developed to extract clusters and cluster changes in multinetwokr systems (Mucha et al., 2010) and recently applied to neuroimaging data sets (Bassett et al., 2011) (Figure 2A).

Unlike other clustering algorithms, this algorithm enabled us to identify network communities (putative functional modules) in brain networks both within and across task states. Using this approach, we identified network communities elicited differentially across tasks (using a low intertask coupling parameter), and we also identified consensus communities present across tasks (using a high intertask coupling parameter). The assignment of brain regions to communities is referred to as a "partition." The coupling parameter determines the extent to which identified partitions are constrained by multiple task states. We were most interested in low coupling parameters, in which all task states are considered separately, and also especially interested in high coupling parameters (identified by the production of a partition stable across additional increases in the coupling parameter), in which all task states are considered together. To examine the relationship between these community partitions and a previously defined resting-state FC community partition (Power et al., 2011) (Figure 2B), we calculated the partition similarity using the Z score of the Rand coefficient (Traud et al., 2011).

We hypothesized that there would be significant differences among the task partitions at low coupling parameters but that they would converge on a consensus partition similar to the resting-state FC community partition at high coupling parameters. Note that the multislice community detection approach forces a single consensus partition at high coupling parameters, but this approach does not require that the consensus partition look like any other particular partition (e.g., a resting-state FC partition). Furthermore, this approach does not require that partitions differentiate from any particular other partition at low coupling parameters.

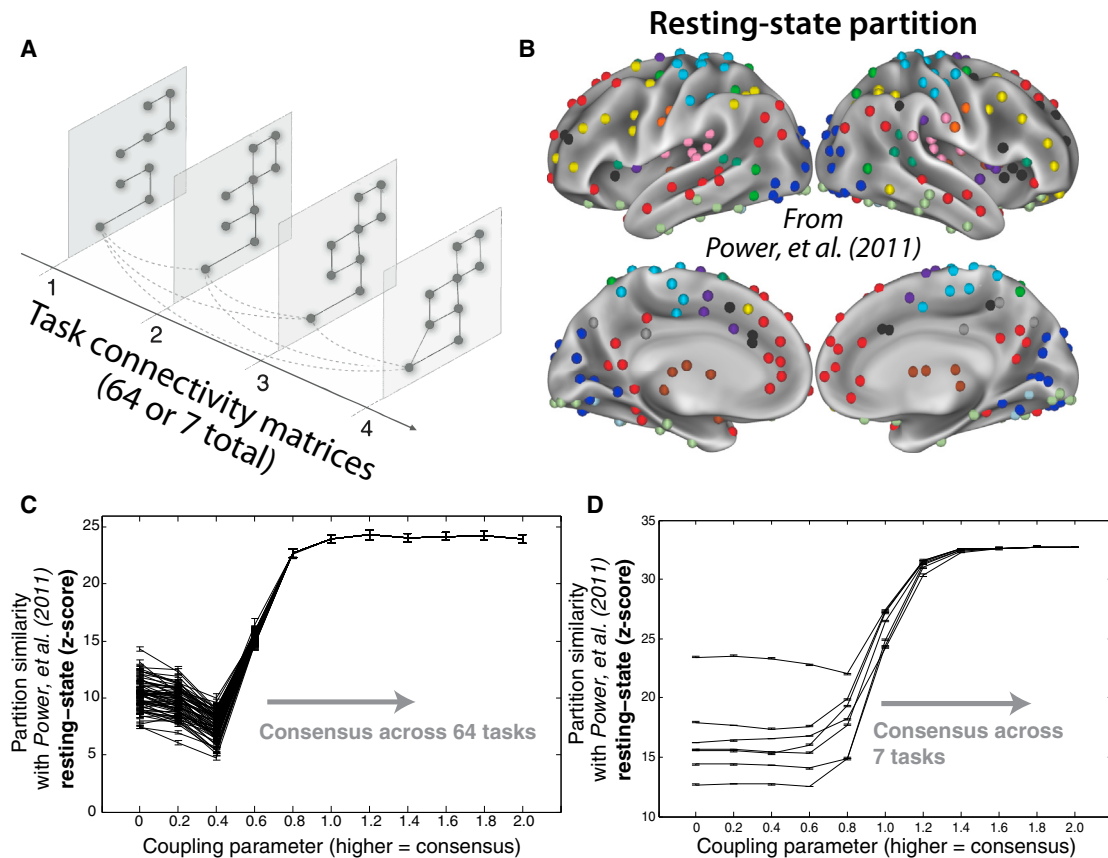


**Figure 2. Multislice Community Detection Reveals a Network Architecture across Tasks Similar to an Independently Identified Resting-State Network Architecture**

(A) Multislice community detection identifies clusters of highly connected nodes, either separately (low coupling parameter) or jointly (high coupling parameter) across multiple states. Adapted from Mucha et al. (2010).

(B) The community partition identified by Power et al. (2011) using independent resting-state data, color coded by community assignment.

(C) Similarity of each task partition to the resting state partition reported in Power et al. (2011). When the coupling parameter is low, changes in community structure across tasks are readily apparent, indicating evoked FC changes. In contrast, as the coupling parameter increases, a consensus partition is identified that is highly similar to an independently identified resting-state FC partition (Power et al., 2011), suggesting the presence of an intrinsic network architecture across tasks. Error bars indicate SEs across subjects.

(D) Similar results in the seven-task data set.

When the coupling parameter was low, allowing greater independence of communities across tasks, significant differences were found in community structure across tasks (Figure 2C). This was found using an ANOVA on partition similarities with a coupling parameter of 0 (see [Experimental Procedures](#) for details):  $F(63,13) = 21$ ,  $p < 0.00001$ . This indicates that the brain's functional network architecture can differ between task states, as implied by previous task FC studies (Bassett et al., 2011; Friston, 2011; Rissman et al., 2004; Cocchi et al., 2013). When coupling parameters were higher, encouraging the algorithm to find common structure across tasks, a single architecture emerged with high similarity to the resting-state network architecture:  $Z = 24$ ,  $p < 0.00001$ . Similar results were obtained in the seven-task data set (Figure 2D). Note that across all tasks, and even with low coupling parameters and thus more variable partitioning (Figure 2C, left), the similarity of task partitioning to resting-state partitioning was high (task with lowest similarity:

$Z = 7$ ,  $p < 0.00001$ ). This indicates that the network architecture present across many task states is also present during rest, signifying the general relevance of resting-state FC to task states.

#### Intrinsic Network Architecture: Resting-State and Multitask Similarity

We used the multislice community approach because of its ability to simultaneously characterize network dynamics in terms of interstate differentiation (at low coupling parameters) and interstate similarity (at high coupling parameters). We next used a simpler approach to better characterize the intrinsic network architecture observed at high coupling parameters. This approach involved building FC matrices of pairwise functional connections separately for multitask and resting-state FC. We equated these two forms of FC for comparison by calculating multitask FC as similarly as possible to how resting-state FC

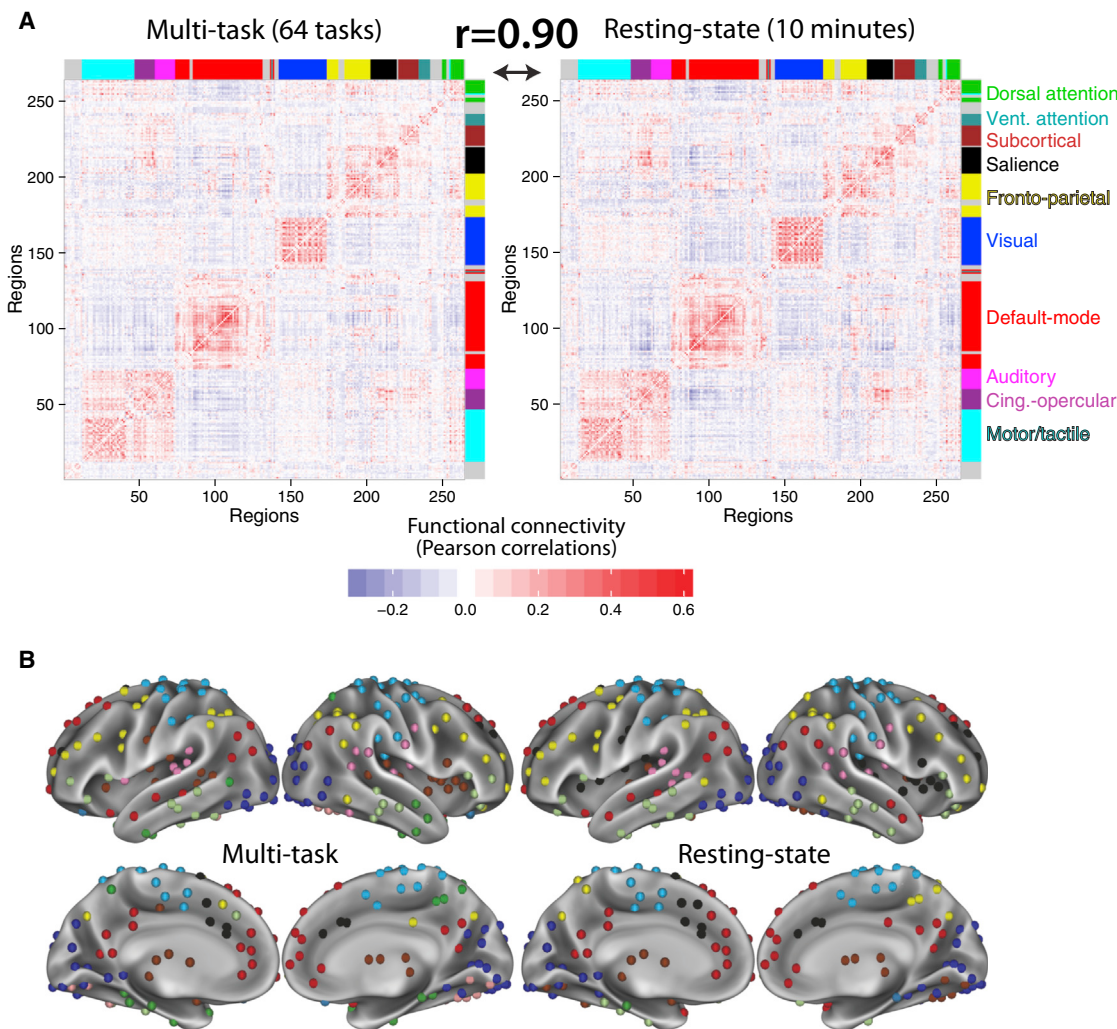


**Figure 3. Multitask Architecture Is Highly Similar to the Resting-State Architecture, Reflecting the Existence of an Intrinsic Network Organization**

(A) Group-averaged multitask and resting-state functional connectivity matrices, with brain regions ordered according to putative functional systems (coded by color bands along the matrix edges) previously identified from resting-state data (Power et al., 2011). Strong intramodule FC demonstrates community structure consistent with functional systems. Multitask FC (left) reflects the central tendency of interregional correlations across tasks, while resting-state FC (right) reflects interregional correlations in spontaneous activity. The high similarity between these two matrices ( $r = 0.90$ ,  $p < 0.00001$ ) suggests that multitask and resting-state FC both reflect an intrinsic functional network architecture.

(B) A standard community detection approach (Blondel et al., 2008) was used to partition multitask and resting-state FC into putative functional brain systems. The partitions were similar to the independently defined resting-state FC partition (Figure 2B):  $Z = 94$  for resting state,  $Z = 79$  for multitask.

was calculated. Specifically, multitask functional connections were calculated as correlations across the concatenated time series of all 64 tasks (excluding rest periods). We thus define the *multitask* matrix as the network organization observed across many task states, estimated from 58 min of task fMRI per subject (Figure 3A, left). As a comparison, we define a *resting-state* matrix using resting-state FC, estimated from 10 min of rest fMRI per subject (Figure 3A, right).

We found that the across-subject mean resting-state FC and multitask FC matrices were highly similar ( $r = 0.90$ ,  $p < 0.00001$ ), supporting the existence of intrinsic FC common across rest and a variety of task states. This result was replicated

in the seven-task data set (Figure 4):  $r = 0.90$ ,  $p < 0.00001$ . Note that the seven-task data set estimates were based on 40 min of task fMRI data and 56 min of rest fMRI data per subject. Together, these results suggest that a highly similar underlying network architecture is present across rest and task.

We hypothesized that the equivalence of multitask FC and resting-state FC was due to resting-state FC reflecting the most frequent (modal) state of a given connection, suggesting each FC value has a “standard” value that tends to remain unchanged across task states and rest. We calculated a multitask modal FC matrix by calculating the mode across all 64 tasks for each connection (Figure 5). Consistent with our hypothesis, the

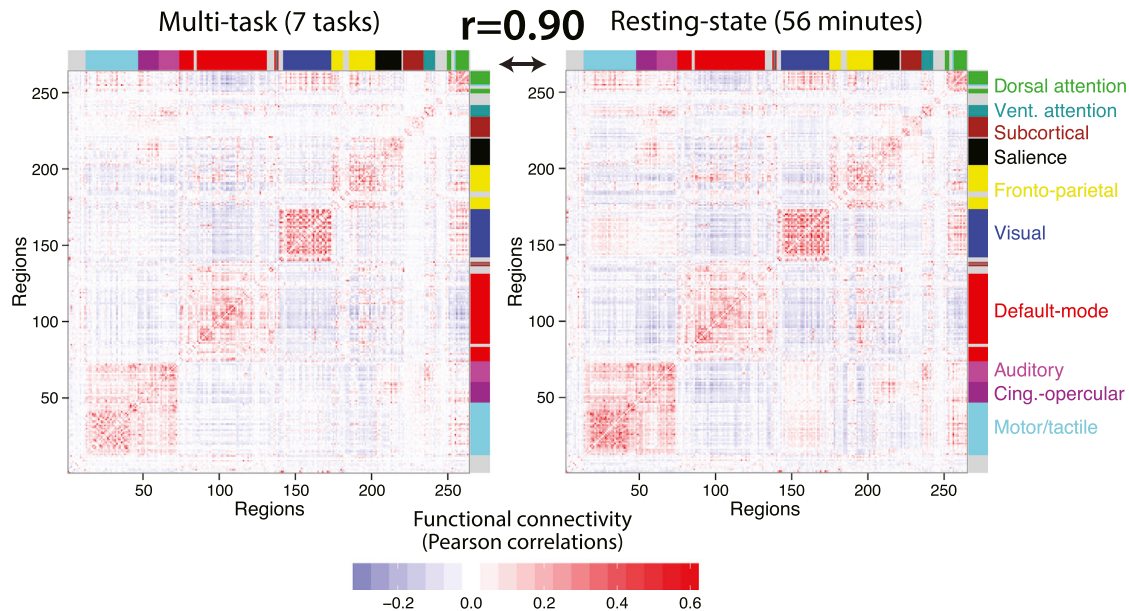


**Figure 4. Multitask Intrinsic FC Is Also Highly Similar to Resting-State FC in the Seven-Task Data Set**

The multitask and resting-state FC comparison analysis was repeated with the seven-task data set, with identical conclusions as with the 64-task data set. Note the high similarity not only between these two matrices, but also their similarity to the matrices from the 64-task data set (Figure 3A).

multitask modal FC matrix was highly correlated with the multitask matrix (64-task data set,  $r = 0.92$ ; seven-task data set,  $r = 0.97$ ). We more directly tested this possibility by comparing the multitask modal FC matrix with the resting-state FC matrix. Though the correlation was lower than with the original multitask matrix it was still highly significant (64-task data set:  $r = 0.83$ ,  $p < 0.00001$ ; seven-task data set,  $r = 0.88$ ,  $p < 0.00001$ ), suggesting intrinsic FC reflects the most frequent state of a given connection. Intuitively, this can be visualized as an approximately Gaussian distribution for each connection across brain states, with a prominent peak reflecting the modal value and suggesting a tendency for the connection's strength to remain stable across states.

We next sought to better characterize the intrinsic network architecture by identifying the network communities present in the resting-state and multitask FC matrices and comparing these partitions to a previously identified resting-state community partition (Figure 2B). A standard algorithm (Blondel et al., 2008) was used to identify communities—groups of regions with stronger within-group FC than expected in a nonparametric null model (see Experimental Procedures for details).

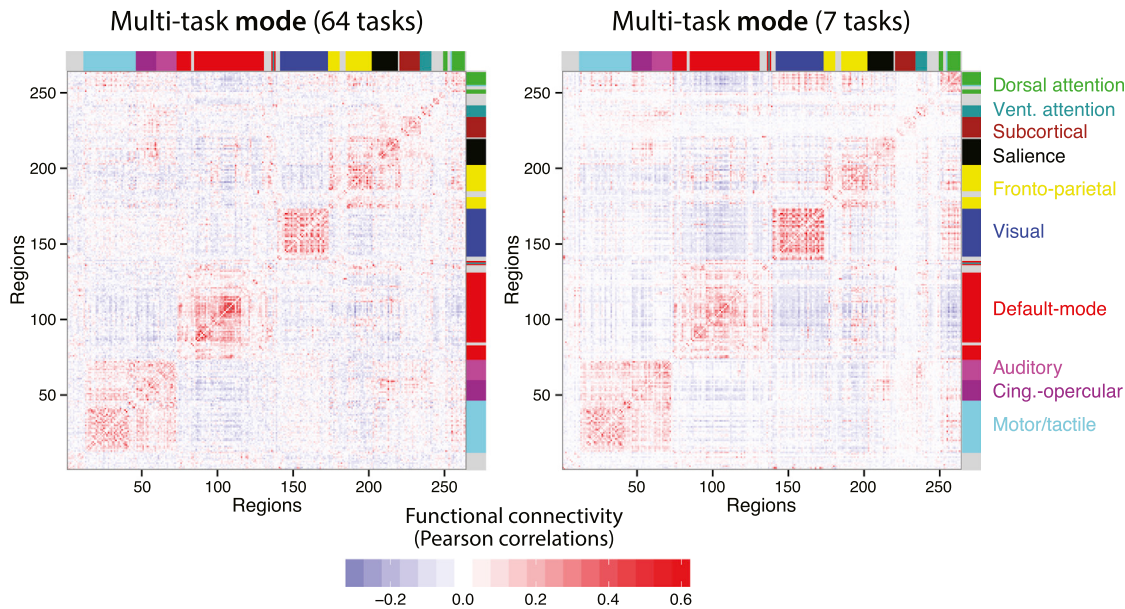
We observed similar network partitions for resting-state FC and multitask FC (Figure 3B):  $Z = 128$ ,  $p < 0.00001$ . Furthermore, the resting-state FC ( $Z = 94$ ,  $p < 0.00001$ ) and multitask FC ( $Z = 79$ ,  $p < 0.00001$ ) partitions were also similar to the partition identified by Power et al. (2011) using independent resting-state data and a distinct community detection approach (Figure 2B). Note that the few observable differences between the partitions in Figure 3B were not stable (i.e., they shifted depending on the exact partitioning parameters chosen) and likely reflect noise in the data given the small number of subjects included in this analysis. These results support the conclusion that there is an intrinsic FC

architecture that is present across rest and a variety of tasks and that this network architecture is largely consistent with known functional systems such as visual, default, and fronto-parietal systems.

#### Intrinsic and Evoked FC: Relative Contributions to Task Network Configurations

The results thus far suggest the existence of both intrinsic and evoked network architectures and that the intrinsic network architecture reflects a standard value for each functional connection across task states. This implies that the intrinsic network architecture continues to shape the brain's overall functional network structure during tasks but that task-specific FC changes are also present. We next assessed the degree to which intrinsic FC and evoked FC contribute to each task's functional network structure (i.e., each task's FC matrix). As before, we primarily utilized FC matrix comparisons. We illustrate these FC matrix comparisons using the seven-task data set (Figure 6), given the better single-task FC estimates due to substantially larger amount of data per task (several minutes each) relative to the 64-task data set (approximately 22 s each). We continue to focus on the seven-task data set whenever single-task FC estimates are involved.

We assessed the relative contribution of intrinsic FC and evoked FC to each task FC matrix by calculating the correlation between the intrinsic FC matrices and each task individually (Figure 6 and Figure S1A available online). As before, we compared whole-brain FC matrices using Pearson correlations, but we now square the resulting  $r$  values to facilitate inferences regarding percent variance explained. We found that the resting-state FC matrix was highly correlated with each individual task on average (mean squared Pearson correlation

**Figure 5. Multitask Modal FC Matrices**

The modal FC values across tasks are visualized for both data sets. This consisted of identifying the most frequently occurring value across all task states for each functional connection.

coefficient [ $r^2$ ] = 0.38,  $t(63) = 153$ ,  $p < 0.00001$ ), as was the multitask FC matrix (mean  $r^2 = 0.46$ ,  $t(63) = 166$ ,  $p < 0.00001$ ). Moreover, we observed that the multitask FC matrix accounted for more of the intertask variance than did the resting-state FC matrix (Student's t test on the Pearson correlation coefficients [ $r$ ] between the reference matrix and the individual task matrices:  $t(63) = 55$ ,  $p < 0.00001$ ). Note that for these comparisons the multitask FC matrix was estimated from 63 tasks: the to-be-compared task was removed from the multitask estimates to remove circularity. We explore the implications of greater similarity of individual tasks to multitask than rest FC further below.

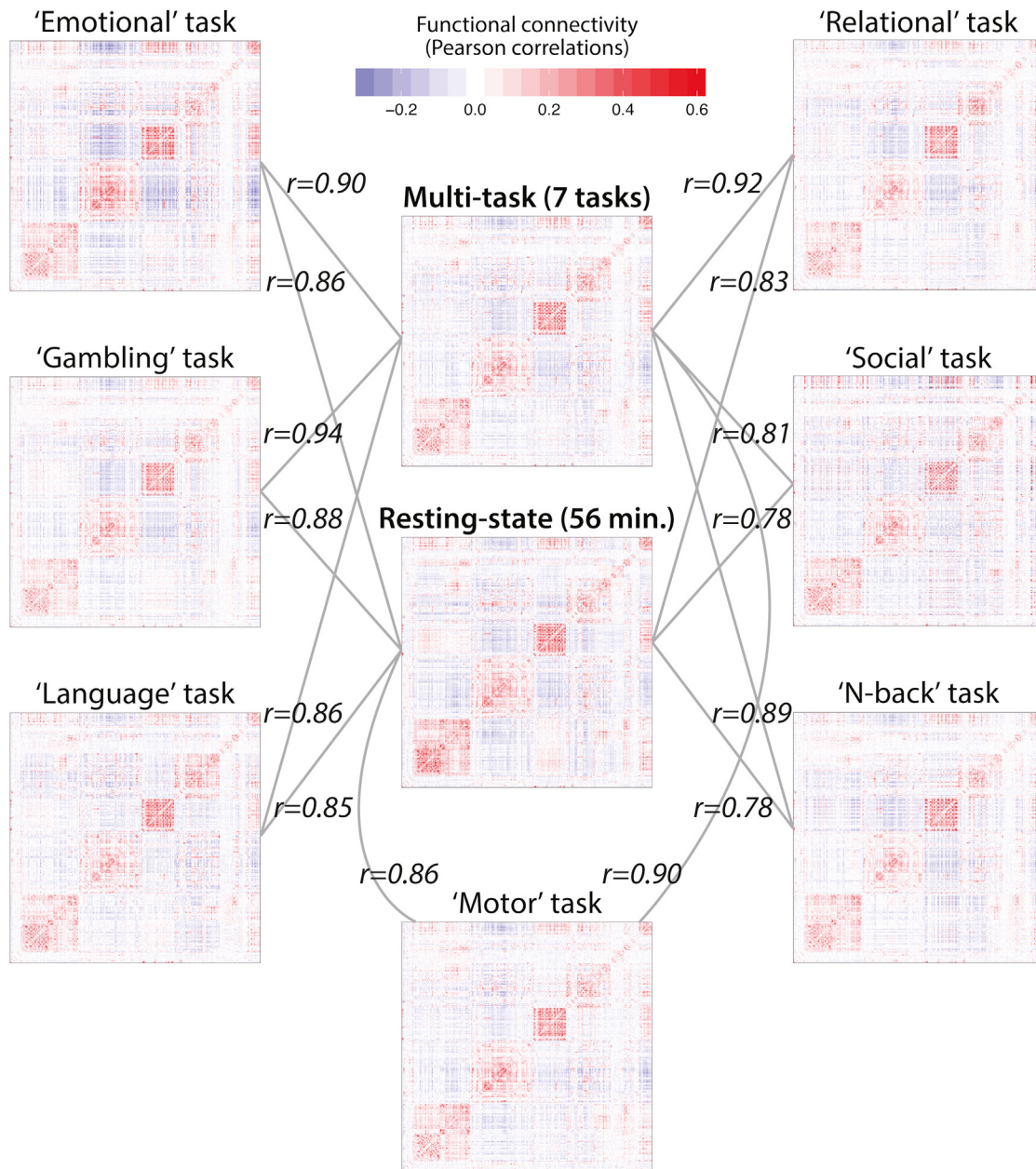
We next asked whether similar results could be obtained from the seven-task data set. Despite large differences between the data sets, our findings in the 64-task data set were also observed in the seven-task data set. Specifically, the resting-state FC matrix was highly correlated with each individual task on average (mean  $r^2 = 0.70$ ,  $t(6) = 26$ ,  $p < 0.00001$ ), as was the multitask FC matrix (mean  $r^2 = 0.81$ ,  $t(6) = 17$ ,  $p < 0.00001$ ). Moreover, we observed that the multitask FC matrix accounted for more of the intertask variance than did the resting-state FC matrix (Student's t test on the Pearson correlation coefficients between the reference matrix and the individual task matrices:  $t(6) = 4$ ,  $p = 0.006$ ). Note that the differences in effect sizes between the data sets was due to differences in the amount of data per task (see **Supplemental Experimental Procedures**), corroborating our decision to focus primarily on the seven-task data set for analyses involving individual task FC estimates.

To further confirm the existence of an intrinsic network architecture across diverse brain states, we used a complementary data-driven approach: principal component analysis on all seven of the task FC matrices. We identified a single principal component that accounted for approximately 85% of the variance

in intertask network architecture (Figure 7A). Consistent with our prior analyses, this component looked very similar to the resting-state FC matrix ( $r = 0.90$ ) (Figure 7B). Furthermore, the weighting of every task on this first component was positive, signifying that the component was present across all tasks. Finally, we assessed the contribution of resting-state FC to this component relative to task FC. We performed a second principal component analysis on eight FC matrices: the seven task FC matrices and one resting-state FC matrix. We again identified a component that accounted for approximately 85% of the variance in interstate network architecture. We controlled for the amount of data by ensuring that the resting-state FC matrix was estimated using the same number of time points as one of the task FC matrices (the "emotional" task). We observed that the first principal component in this larger decomposition was most highly weighted to the resting-state FC matrix, with a weight of 0.42 (next highest, 0.41; average weight of the seven tasks, 0.34) (Figure 7C). These results complement our prior analyses by again demonstrating the existence of an intrinsic functional network architecture across task states and by suggesting that this architecture is similar to all task-specific FC network architectures as well as the resting-state FC network architecture.

#### Task-Evoked Differences from Rest Reveal Task-General Network Changes

We next used a distinct approach to better determine the amount of FC modification relative to rest for each of the seven tasks. Rather than using matrix correlations, we tested each connection independently using t tests ( $p < 0.05$ , false discovery rate corrected for multiple comparisons). We then calculated the percentage of connections significantly changed from rest

**Figure 6. Comparison of Intrinsic FC with Individual Task FC**

Each of the seven-task data set task FC matrices is visualized along with the multitask and resting-state FC matrices. Note that the Pearson correlation coefficients ( $r$ ) for comparisons with the multitask FC matrix were based on six tasks: the to-be-compared task was removed from the multitask estimates to remove circularity. These results illustrate the presence of intrinsic FC (a similar FC pattern across all tasks), along with evoked FC changes across tasks.

(Figure 8A), indicating that 38.98% of connections were altered on average (minimum, 33.92%; maximum, 48.37%). This is consistent with the result obtained using matrix correlations reported above, despite reporting in terms of the number of estimated changes rather than variance explained. Together these results suggest most functional connections are not changed significantly from the resting-state network architecture during a given task state. Further confirming the generally small amount of change from rest, the average absolute value FC change from

rest across all tasks and connections was 0.04 (0.07 among significantly changed connections).

We next explored the properties of the relatively few (but likely functionally important) task-evoked FC changes from rest. We began by plotting each functional connection's change from rest versus its connection strength at rest (Figure 8B). A negative relationship was apparent, indicating that connections with higher resting-state FC tend to decrease during tasks, while connections with lower resting-state FC tend to increase during

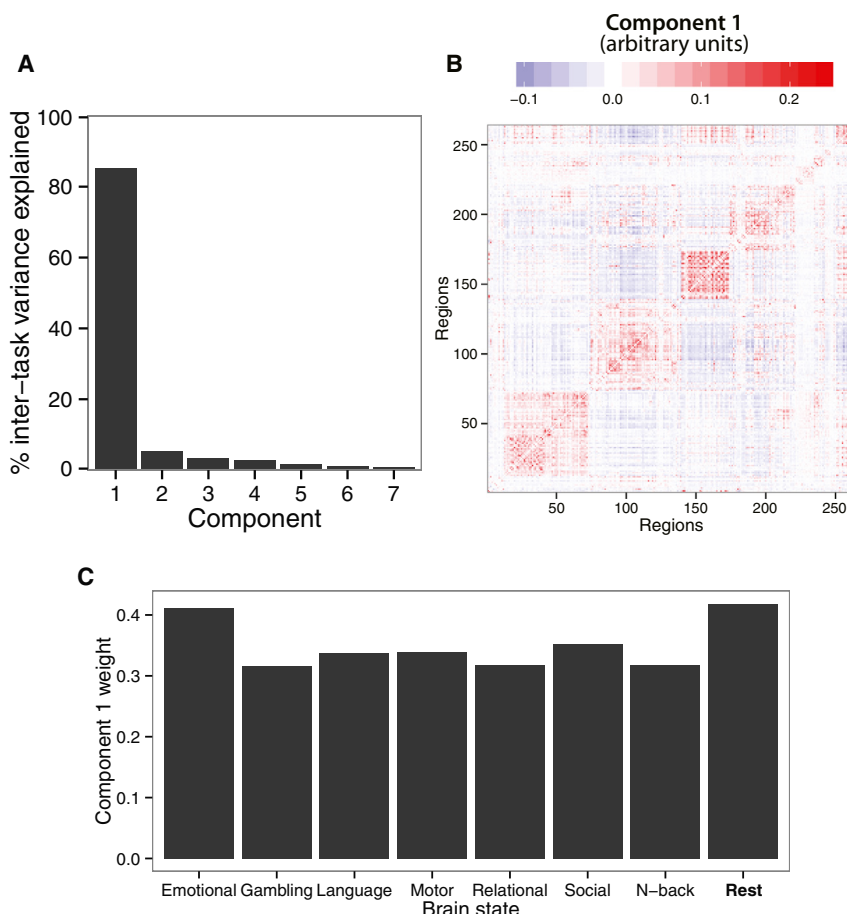


**Figure 7. A Single Principal Component Accounts for Most Intertask Network Architecture Variance**

(A) The first principal component across the seven task FC matrices accounted for 85% of the intertask FC matrix variance.

(B) The first principal component (from A) was highly similar to the resting-state FC matrix ( $r = 0.90$ ).

(C) Another principal component analysis additionally included the resting-state FC matrix (for a total of eight FC matrices). The first principal component (again accounting for 85% of variance) loaded most heavily on the resting-state FC matrix, suggesting this component is most related to the network architecture at rest (although it was also related to all individual task FC architectures).

relatively similar result ( $r = 0.31$ ,  $p < 0.00001$ ) despite major differences between data sets. Within-community connections for both the seven-task (mean within-community change,  $-0.04$ ) and the 64-task (mean within-community change,  $-0.02$ ) tended to decrease for multitask FC relative to resting-state FC.

## DISCUSSION

The present findings reframe resting-state FC and task FC in terms of intrinsic versus evoked network architectures. This framework may facilitate an integrated understanding across the subfields

tasks. This was the case for all seven tasks ( $r$  values of  $-0.24$ ,  $-0.66$ ,  $-0.48$ ,  $-0.53$ ,  $-0.61$ ,  $-0.38$ , and  $-0.58$ ; all  $p < 0.00001$ ).

We next plotted the significant changes from rest for each task, separately for increases and decreases (Figure 8C). This revealed a complex pattern, with many connections being changed across all or most tasks. Notably, there was a strong tendency for within-community connections to decrease (percent of significant within-community FC changes that were decreases, 79%), while there was a small tendency toward between-community connections increasing (percent of significant between-community FC changes that were increases, 51%). This is consistent with the observed negative correlations between task-evoked FC changes and resting-state FC, given that the communities were defined based on strong resting-state FC. Note that even though strong positive connections tended to decrease, they almost always stayed strongly positive during tasks (Figure 6).

We next summarized consistent across-task FC changes from rest by subtracting the multitask FC matrix by the resting-state FC matrix (Figure 8D). The similarity between this FC matrix and consistent FC changes across tasks in Figure 8C suggests that the above-mentioned results demonstrating greater individual-task FC similarity to multitask than rest FC (Figures 6 and S1) was due to consistent task FC changes from rest. We also ran this analysis with the 64-task data set (Figure 8E), revealing a

of neuroscience that currently focus separately on either resting-state or task FC. For instance, this account suggests functional brain systems are defined by a stable intrinsic network architecture that is present across rest and tasks (Figures 2 and 3), establishing an intimate link between resting-state FC and task FC. The intrinsic structure is dominant: we found that FC strengths typically stay unchanged from rest once a task begins (Figures 5 and 6) and that resting-state FC accounts for most of the brain's functional network architecture during individual tasks (Figures 7 and S1). This suggests that while statistically significant changes in FC occur across tasks (Figures 2 and 8), these changes are relatively small (although likely important functionally) overall. We further found that task-evoked FC changes from rest are often similar to one another, suggesting the existence of a task-general network architecture (Figure 8). Together, these results suggest the functional network architecture present during a given task is shaped primarily by the intrinsic network architecture and secondarily by a limited set of task-general and task-specific evoked FC changes.

## Intrinsic and Evoked Network Architectures Jointly Shape Task FC

Previous findings identified similarity between resting-state FC and task FC for a small number of brain regions and tasks (Biswal et al., 1995; Fair et al., 2007; Fox et al., 2007; Greicius et al.,

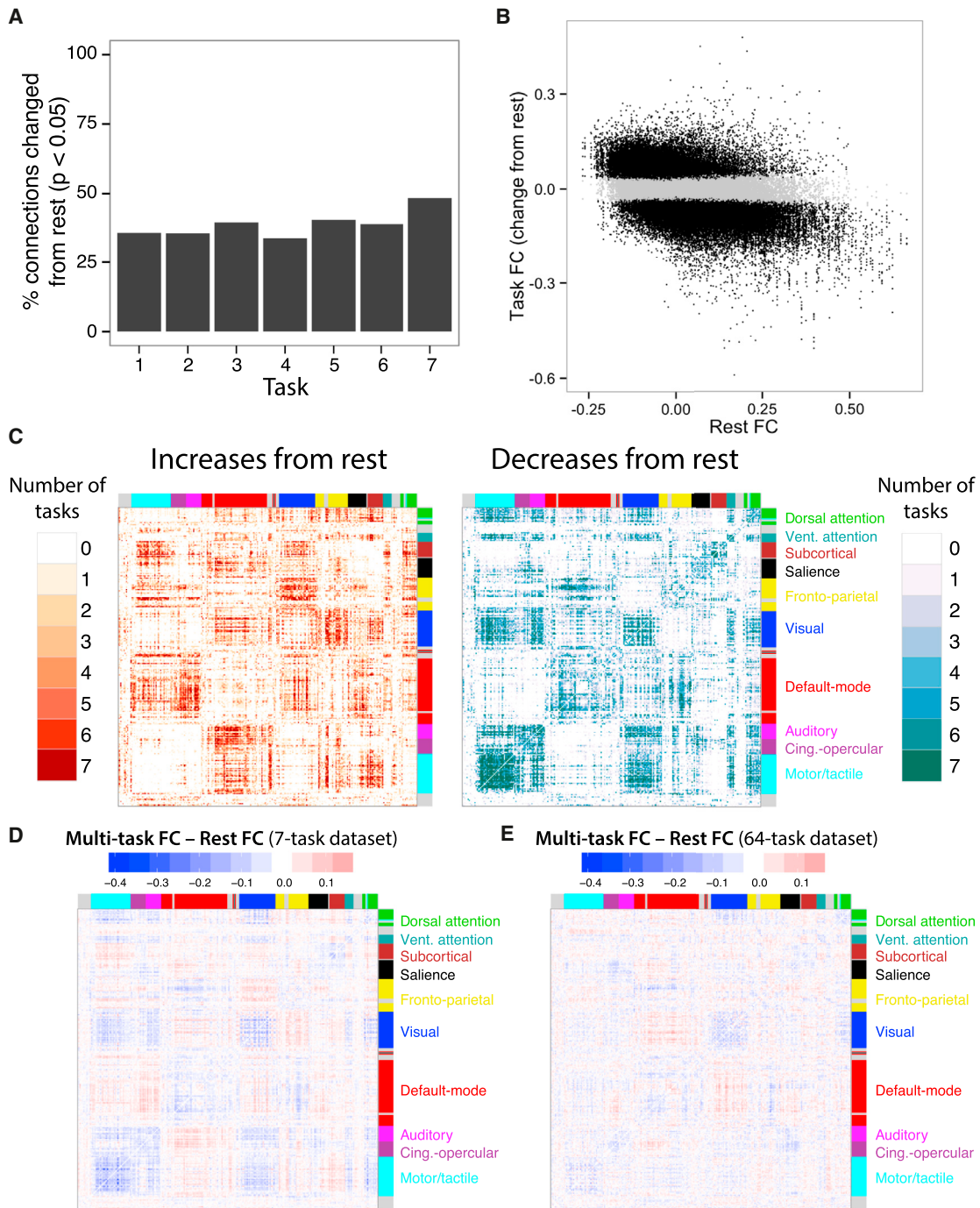


**Figure 8. Task-Evoked FC Changes from Rest Reveal a Task-General Dynamic Network Architecture**

- (A) Each task's whole-brain FC matrix was compared to the resting-state FC matrix (from Figure 4). The task order is the same as in Figure 1B.
- (B) All task FC changes from rest are plotted (across all seven tasks) versus their resting-state FC values. Significant changes from rest are black, while nonsignificant changes are gray. Most of the connections (61%) were nonsignificant. The correlation between task FC changes and rest FC was negative for all seven tasks (mean  $r = -0.49$ ).
- (C) The count of how many tasks involved significant changes from rest plotted for each connection. Many connections changed for all seven tasks (11% of changed connections).
- (D) Differences between the multitask FC matrix and resting-state FC matrix (left versus right sides of Figure 4), summarizing general changes from rest that are common across tasks.
- (E) The same analysis for the 64-task data set, on the same scale as (D). The matrices here and in (D) were relatively similar (despite major differences between data sets) ( $r = 0.31$ ,  $p < 0.00001$ ).

2003). More recently, studies examining many regions have emphasized differences between resting-state FC and FC during a small number of tasks (Buckner et al., 2013; Hasson et al., 2009; Mennes et al., 2013). This suggested that resting-state FC may not be informative regarding tasks (Buckner et al., 2013), yet we identified a whole-brain intrinsic network architecture across a wide variety of tasks and rest, suggesting resting-state FC is relevant to task states. This is broadly consistent with previous studies showing correlations between individual differences in resting-state FC and task performance (Cole et al., 2011, 2012; Kelly et al., 2008; van den Heuvel et al., 2009) and with studies that identified correlations between resting-state FC and task coactivation patterns (based on neuroimaging meta-analysis) (Laird et al., 2013; Smith et al., 2009). Importantly, the present results provide a potential explanation for these observations: resting-state FC may relate to behavior and task coactivation patterns because the intrinsic network architecture shapes FC during both rest and a wide variety of task states.

This perspective suggests that the intrinsic network architecture influences all brain activity, including task-evoked activation patterns. The clearest evidence for this comes from the similarity of task-evoked activation patterns to the intrinsic network architecture (Laird et al., 2013; Smith et al., 2009; Ritchey et al., 2014), which suggests a strong association between intrinsic FC and task activation. Thus, it may be that even if observed FC correlations during tasks are largely driven by spontaneous activity (Fox et al., 2007), the intrinsic network architecture nonetheless shapes task-evoked activation patterns. The present results suggest that both spontaneous activity and evoked activity may flow through the same functional network architecture, with relatively minor changes to this architecture across different contexts. It will be important for future research to make more direct links between task-evoked activations, behavior, and the intrinsic functional network architecture in order to better determine the extent to which the intrinsic architecture shapes both spontaneous and task-evoked functionality.

One major reason for current interest in resting-state FC is the possibility that it can be used to identify a universal intrinsic network architecture present across most or all brain states. As outlined above, preliminary evidence for such universality came from studies relating meta-analytic task activation patterns to rest FC (Laird et al., 2013; Smith et al., 2009). We went beyond these findings to determine that the actual FC architectures during a variety of individual task states (rather than covariance of activation patterns across tasks/studies) are highly similar to the resting-state FC architecture. We found that this intrinsic network architecture was not fixed, however. Instead, the intrinsic network architecture appeared to be a “standard” state of the human brain’s functional network, with task demands having a moderate effect on this state when considered in terms of overall brain organization (Figures 7 and 8A). These results suggest that investigating resting-state FC is an efficient means for understanding the human brain’s functional organization across a wide variety of brain states but that full understanding will require the characterization of individual brain states.

Indeed, despite their moderate effect on overall brain organization, evoked FC changes are likely of primary importance for

a variety of functional questions. For instance, the contribution of network organization to adaptive cognition likely relies on task-specific updates. This is consistent with recent findings indicating that a fronto-parietal system’s FC updates are strongly related to current task demands (Cole et al., 2013). Importantly, such findings are consistent with the present results, which indicate that a relatively small number of connections are changed during task performance, since only a small number of pathways are likely involved in any given task context (e.g., from a particular representation in visual cortex to a particular finger representation in motor cortex during a visual-motor task).

### Task-Evoked Changes from Rest Reveal a Task-General Dynamic Architecture

In addition to a standard network architecture, the brain’s functional network architecture during a given task appears to reflect (1) task-specific evoked FC and (2) task-general evoked FC. We identified this task-general network architecture in several ways, perhaps most straightforwardly as the difference between the multitask FC matrix and the resting-state FC matrix (Figure 8D). This revealed a complex set of FC changes, with a prominent pattern of decreased within-system FC during task performance. It will be important for future research to determine what this pattern means and why it is so consistent across diverse task states.

One possibility is that this effect is due to some difference in electrophysiological brain rhythms during resting state relative to task. For instance, electrophysiological alpha rhythms that are consistently present during rest (Buzsáki, 2006) may indirectly result in increased synchrony in the blood-oxygen-level-dependent signal, such that shifts to other frequencies during task performance decrease fMRI-based FC. Another possibility is that task performance requires a partial breakdown of network communities (reflected in decreased within-system FC), such that activity can better flow between systems with diverse functions.

Another notable task-general pattern is the increase between the visual system and fronto-parietal, default-mode, and subcortical systems. It will be important to determine the significance of this pattern. The consistent FC decrease between fronto-parietal and default-mode systems is also notable, given evidence that the fronto-parietal system contributes to decreases in default-mode activity during a variety of tasks (Anticevic et al., 2012; Raichle, 2010).

More broadly, the observation of a task-general network architecture suggests that multitask FC might better predict the functional brain architecture in a wide variety of states than resting-state FC. Consistent with this conclusion, the multitask FC architecture was more correlated with most individual task FC architectures than the resting-state FC architecture, for both data sets (Figures 6 and S1A). It may be, however, that the task-general architecture is actually a modification of the resting-state architecture, which better reflects the “true” intrinsic network architecture given that rest involves especially low metabolic demand (Raichle et al., 2001). Consistent with this, we found that rest FC was most related to a network architecture component common across all tested brain states (Figure 7). Overall these results suggest that the resting-state

network architecture better reflects the intrinsic architecture, which is consistently modified by the task-general architecture across a wide variety of tasks.

### Limitations

The present work involves several limitations worth noting. First, while our study investigates an especially large sample of task states per subject, this sample is nonetheless small relative to the virtually infinite variety of possible tasks. However, our results were similar across two data sets with highly distinct sets of tasks, suggesting these results will generalize to a wide variety of other tasks as well. Second, we used a limited set of 264 regions of interest to estimate FC throughout the brain (Power et al., 2011). We used this set of regions because it sampled from every major brain system, was estimated using independent data (reducing potential circularity or biases from overfitting in our analyses [Kriegeskorte et al., 2009]), and came with an independently identified node community partition (again, to reduce potential biases). Third, less data per task was available relative to many task FC studies, potentially reducing the reliability of our results. We were able to find statistically significant differences across task functional connections based on inter-subject variance (Figures 2 and 8), suggesting results were nonetheless fairly reliable across subjects. Furthermore, most results were similar across the two data sets despite substantial differences in the amount of data per task.

### Future Directions

It will be important for future research to identify the forces that shape the intrinsic network architecture. One likely possibility is that structural connectivity shapes spontaneous and evoked activity flow through brain networks (Adachi et al., 2012; Goñi et al., 2014), resulting in similar time series correlations across rest and task states. Importantly, however, structural connectivity cannot fully account for resting-state FC (Goñi et al., 2014). This suggests that synaptic efficacy—the tendency for one neuron to fire in response to another anatomically connected neuron—also plays a role in shaping the intrinsic network architecture. Consistent with this possibility, resting-state functional connections change with task training (Lewis et al., 2009), suggesting the intrinsic network architecture partially reflects learning (possibly via synaptic modifications) from previous task experiences. The present results suggest this learning may be Hebbian in nature (Hebb, 1949). This is because resting-state FC looks similar to multitask FC (Figures 2 and 3), which forms a consensus across a broad sampling of task experiences similar to how Hebbian learning would, given the many tasks implemented in daily life. It will be important for future research to more directly investigate the role of Hebbian-like learning in shaping the intrinsic network architecture, perhaps using task training in combination with rest, task, and multitask FC techniques.

It will also be important to identify the exact neuronal mechanisms by which evoked FC is altered across tasks. For example, this may occur via short-term plasticity (Yao et al., 2007; Zucker and Regehr, 2002) or via altered synchrony of oscillations among neuronal populations (Buzsáki and Draguhn, 2004; Fries, 2005), possibly coordinated by the fronto-parietal

control system (Cole et al., 2013; Miller and Cohen, 2001; Sakai, 2008). Indeed, recent results suggest the fronto-parietal system consists of flexible hubs—brain regions with especially high concentrations of evoked FC dynamics with a variety of brain systems (Cole et al., 2013). It will be critical for future research to further characterize the role of fronto-parietal and related systems in top-down control of whole-brain network reconfiguration as well as the role of distributed and self-organizing processes that are independent of these systems.

The characterization of stable and dynamic FC in the present study also suggests the need to reconcile these findings with evidence that resting-state FC is not stable over time (Hutchison et al., 2013). For instance, it will be important to determine whether the intrinsic network architecture identified here is also prominent across temporal windows during rest, much like was observed here across task states. Furthermore, it will be important to test whether the connections that changed the most across tasks here are also those that change the most across temporal windows during rest. Such a finding would suggest the “flexibility” of a functional connection is a stable property of that connection and therefore something that could be used to predict brain dynamics across a variety of states.

### Conclusions

In this report we found that many of the interregion temporal relationships observed during rest are also present during a wide variety of tasks. This intrinsic network architecture reflects the most frequent state of each functional connection across task states, suggesting it is a standard state of the brain. Furthermore, changes from the intrinsic FC network architecture tend to be limited, as the intrinsic network architecture accounts for more than half of the variance in the functional network structure during any given task. When task-evoked differences are present, however, they consist of task-general and task-specific changes from rest. Together, these results bridge perspectives emphasizing either intrinsic FC or task-evoked FC, suggesting task FC is composed primarily of intrinsic FC and secondarily of task-evoked FC. Thus, this work provides a framework for future studies to characterize FC during tasks in terms of both intrinsic FC identified using resting states and evoked FC identified across tasks and in particular task contexts.

### EXPERIMENTAL PROCEDURES

#### Data Collection

Two fMRI data sets were collected. We collected the first data set on a 3T Siemens Tim TRIO, with 15 right-handed participants (eight male, seven female), aged 19–29 years (mean age, 22 years). Participants were recruited from the University of Pittsburgh (Pittsburgh, PA) and surrounding area. All participants gave informed consent. Further details regarding participant selection for this data set can be found elsewhere (Cole et al., 2010). Thirty-eight transaxial slices were acquired every 2000 ms (field of view, 210 mm; echo time, 30 ms; flip angle, 90°; voxel dimensions, 3.2 mm<sup>3</sup>), with a total of 300 echo-planar imaging volumes collected for the rest run and 216 volumes per task run. Siemens' implementation of generalized autocalibrating partially parallel acquisition was used to double the image acquisition speed (Griswold et al., 2002). Ten minutes of rest (eyes open with fixation) fMRI data were collected, followed by ten task fMRI runs involving 64 tasks (four previously practiced, 60 novel) (Cole et al., 2010). The tasks were presented in short

blocks (average duration, 22 s) consisting of task instructions (4 s) followed by three trials (2 s each). Each trial event was followed by a variable 2–6 s delay, while each task block was followed by a variable 12–16 s delay.

The second data set was collected as part of the Washington University-Minnesota Consortium Human Connectome Project (Van Essen et al., 2013). Participants were recruited from Washington University (St. Louis, MO) and the surrounding area. All participants gave informed consent. The data used were from the first and second quarter releases, consisting of data from 139 participants. Data from 21 subjects were not used because one or more of the data runs were not collected for these subjects, such that data from 118 subjects were included in the analyses. Whole-brain echo-planar imaging acquisitions were acquired with a 32 channel head coil on a modified 3T Siemens Skyra with time to repetition (TR) = 720 ms, time to echo = 33.1 ms, flip angle = 52°, bandwidth = 2,290 Hz/pixel, in-plane field of view = 208 × 180 mm, 72 slices, and 2.0 mm isotropic voxels, with a multi-band acceleration factor of 8 (Uğurbil et al., 2013). Data were collected over 2 days. On each day 28 min of rest (eyes open with fixation) fMRI data across two runs were collected (56 min total), followed by 30 min of task fMRI data collection (60 min total). Each of the seven tasks was completed over two consecutive fMRI runs. Resting-state data collection details for this data set can be found elsewhere (Smith et al., 2013), as can task data details (Barch et al., 2013).

### Data Preprocessing

In brief, the 64-task data set preprocessing consisted of standard functional connectivity preprocessing (typically performed with resting-state data), with several modifications given that analyses were also performed on task-state data. Resting-state and task-state data were preprocessed identically in order to facilitate comparisons between them. We performed slice timing correction, motion correction, removal of the first five volumes of each run, normalization to a Talairach template, within-run intensity normalization to a whole-brain mode value of 1,000, linear trend removal for each run, regression of nuisance variables (24 motion parameters, ventricle, whole-brain, and white matter signals, along with signal derivatives) using linear regression, and spatial smoothing (6 mm full width at half maximum). Note that the main results were broadly similar with and without whole-brain (global) signal regression. Unlike with standard resting-state functional connectivity preprocessing, a lowpass temporal filter was not applied, given the possible presence of task signals at higher frequencies than the relatively slow resting-state fluctuations. Data volumes with high motion were censored to reduce potential motion artifacts (Power et al., 2014). We used a frame-wise displacement threshold of 0.5, above which a given volume would be removed. This threshold was chosen to be similar to previously chosen thresholds, while also allowing at least five volumes per subject for most tasks. Note that most tasks included well above this number of volumes, and only one task (for one subject) was removed from further analysis because the number of remaining volumes fell below five.

We sought to preprocess the seven-task data set in a similar manner as the 64-task data set, although some differences were necessary due to differences in data collection methods. For instance, nonlinear warping was required to correct spatial distortions in this data set. This and related corrections (spatial normalization to a template, motion correction, intensity normalization) were already implemented in a minimally processed version of the seven-task data set described elsewhere (Glasser et al., 2013). With the volume (rather than the surface) version of the minimally preprocessed data, we used AFNI (Cox, 1996) to additionally remove nuisance time series (motion, ventricle, whole-brain, and white matter signals, along with their derivatives) using linear regression, remove the linear trend for each run, and spatially smooth the data (4 mm full width at half maximum). Unlike the 64-task data set, motion censoring was not applied given relatively minimal movement by participants and a desire to see whether replication of results would be possible without motion censoring. In order to make this data set comparable to the 64-task data set, the data were temporally downsampled (as the last step of preprocessing) by averaging data from every three consecutive volumes (making a 2,160 ms TR, close to the 2,000 ms TR in the 64-task data set). This had an effect similar to a mild low-pass temporal filter on the data (removing frequencies above 0.46 Hz).

Note that we performed the main multitask FC to rest FC comparison (Figure 4) without downsampling the seven-task data set as described above, indicating that the downsampling preprocessing step had only minimal effect on the results. Specifically, the resting-state FC matrix comparison to the multitask FC matrix involved almost identical results with ( $r = 0.89899$ ) and without ( $r = 0.89872$ ) downsampling. Further confirming this conclusion, the resting-state FC matrix was highly similar with and without downsampling ( $r = 0.995$ ). This was also true for the multitask FC matrix ( $r = 0.991$ ).

Data were sampled from a set of 264 brain regions (rather than individual voxels) in order to make inferences at the region and systems level. This particular set of regions was used rather than anatomically defined sets of regions in order to reduce the chance of combining signal from multiple functional regions (Wig et al., 2011). These brain regions were identified using a combination of resting-state functional connectivity parcellation (Cohen et al., 2008) and task neuroimaging meta-analysis (Power et al., 2011). A consensus partition across the originally reported threshold-specific partitions was used (Cole et al., 2013). Data were summarized for each region by averaging signal in all voxels falling inside each region.

Preprocessing was carried out using FreeSurfer (Fischl, 2012) and custom code in MATLAB 2012b (MathWorks) for the 64-task data set and AFNI (Cox, 1996) for the seven-task data set (using the minimally preprocessed version of the data [Glasser et al., 2013]). Further analysis was carried out with MATLAB 2012b and R 2.15.1 (The R Foundation for Statistical Computing).

### FC Estimation

We estimated FC using Pearson correlations between time series from all pairs of brain regions (all computations used Fisher's Z-transformed values, which were reconverted to r values for reporting purposes). This was straightforward for resting-state data, as there were no additional steps after preprocessing prior to calculating these correlations. For task data, we sought to suppress or remove influences of (across-trial mean) task-related activations on task-related changes in functional connectivity. This involved standard general linear model regression of task events, followed by use of the residuals from these regression models for estimating task FC, as done previously (Cole et al., 2013; Fair et al., 2007). Note, however, that we found this task regression step had only minimal effects on the results. See the *Supplemental Experimental Procedures* for details.

### Multislice Community Detection

The categorical version of a multislice community detection algorithm (Jutla et al., 2011; Mucha et al., 2010) was applied to each subject's set of task FC matrices. This version of the algorithm considers each state of the modeled graph categorically (each network is an independent sample) rather than in a sequential order (wherein each network is related to the other networks by an ordinal variable like time). The algorithm was applied with a default structural resolution parameter of 1, and the intertask coupling parameter was varied from 0 to 2 in 0.2 increments (for methodological and algorithmic details, see Bassett et al., 2013a). Similar to previous applications to neuroimaging data sets, the algorithm was run with 100 random optimizations each time (Bassett et al., 2011, 2013a, 2013b; Doron et al., 2012). To identify a representative partition, several consensus algorithms exist (Bassett et al., 2013a; Doron et al., 2012; Lancichinetti and Fortunato, 2012). Similar to Doron et al. (2012), we identified the optimization most similar (as defined by the maximum pairwise Z score of the Rand coefficient [Traud et al., 2011]) on average to the other 99 optimizations used for subsequent analysis. We then plotted the similarity (Traud et al., 2011) of each community partition to a previously defined resting-state FC community partition (Cole et al., 2013; Power et al., 2011) for each intertask coupling parameter (Figure 2B).

### Partition Similarity ANOVA

An ANOVA was run on the partition similarities estimated when the coupling parameter was 0. The dependent variable was partition similarity (i.e., the partition similarity Z scores [Traud et al., 2011]), while the categorical variables were task number ( $n = 64$ ) and subject number ( $n = 15$ ). Task number was a fixed effect, while subject number was a random effect. We reported the main effect of task number.

**Multitask FC Estimation**

This analysis involved removing all interblock rest periods from all regions' time series, followed by computing pairwise temporal correlations across all concatenated task periods. Multitask modal FC estimation involved calculating FC for each task separately, rounding functional connections to the nearest 0.01, and then identifying the most frequent FC value across the tasks for each connection. Modal values that occurred only once across tasks for a given subject were removed, and any ties (i.e., values with the same frequency) were resolved by taking the median of the tied values. Modal values were then averaged across subjects for reporting. The modal analysis can be interpreted as asking, "If FC values repeated across tasks, did they tend to look like resting-state FC values"?

**FC Matrix Comparison**

We compared FC matrices by taking the upper triangle of each matrix (i.e., excluding self-connections and redundant connections), applying a Fisher's Z-transform to the FC values, and computing a Pearson correlation on the resulting vectors of FC values.

**Static Community Detection**

See [Supplemental Experimental Procedures](#).

**SUPPLEMENTAL INFORMATION**

Supplemental Information includes Supplemental Experimental Procedures and one figure and can be found with this article online at <http://dx.doi.org/10.1016/j.neuron.2014.05.014>.

**ACKNOWLEDGMENTS**

We thank Timothy Laumann and Takuya Ito for helpful conversations during preparation of this manuscript. Data were provided in part by Walter Schneider's laboratory at the University of Pittsburgh. Data were also provided in part by the Human Connectome Project, Washington University-Minnesota Consortium (principal investigators David Van Essen and Kamil Ugurbil; 1U54MH091657) funded by the 16 NIH institutes and centers that support the NIH Blueprint for Neuroscience Research; and by the McDonnell Center for Systems Neuroscience at Washington University. Our work was supported by NIH award K99/R00 MH096801 (M.W.C.). The content is solely the responsibility of the authors and does not necessarily represent the official views of the NIH.

Accepted: May 6, 2014

Published: July 2, 2014

**REFERENCES**

- Adachi, Y., Osada, T., Sporns, O., Watanabe, T., Matsui, T., Miyamoto, K., and Miyashita, Y. (2012). Functional connectivity between anatomically unconnected areas is shaped by collective network-level effects in the macaque cortex. *Cereb. Cortex* 22, 1586–1592.
- Anticevic, A., Cole, M.W., Murray, J.D., Corlett, P.R., Wang, X.-J., and Krystal, J.H. (2012). The role of default network deactivation in cognition and disease. *Trends Cogn. Sci.* 16, 584–592.
- Barch, D.M., Burgess, G.C., Harms, M.P., Petersen, S.E., Schlaggar, B.L., Corbetta, M., Glasser, M.F., Curtiss, S., Dixit, S., Feldt, C., et al.; WU-Minn HCP Consortium (2013). Function in the human connectome: task-fMRI and individual differences in behavior. *Neuroimage* 80, 169–189.
- Bassett, D.S., Wymbs, N.F., Porter, M.A., Mucha, P.J., Carlson, J.M., and Grafton, S.T. (2011). Dynamic reconfiguration of human brain networks during learning. *Proc. Natl. Acad. Sci. USA* 108, 7641–7646.
- Bassett, D.S., Porter, M.A., Wymbs, N.F., Grafton, S.T., Carlson, J.M., and Mucha, P.J. (2013a). Robust detection of dynamic community structure in networks. *Chaos* 23, 013142.
- Bassett, D.S., Wymbs, N.F., Rombach, M.P., Porter, M.A., Mucha, P.J., and Grafton, S.T. (2013b). Task-based core-periphery organization of human brain dynamics. *PLoS Comput. Biol.* 9, e1003171.
- Biswal, B., Yetkin, F.Z., Haughton, V.M., and Hyde, J.S. (1995). Functional connectivity in the motor cortex of resting human brain using echo-planar MRI. *Magn. Reson. Med.* 34, 537–541.
- Biswal, B.B., Mennes, M., Zuo, X.-N., Gohel, S., Kelly, C., Smith, S.M., Beckmann, C.F., Adelstein, J.S., Buckner, R.L., Colcombe, S., et al. (2010). Toward discovery science of human brain function. *Proc. Natl. Acad. Sci. USA* 107, 4734–4739.
- Blondel, V.D., Guillaume, J.-L., and Lambiotte, R. (2008). Fast unfolding of communities in large networks. *J. Stat. Mech.* 2008, P10008.
- Buckner, R.L., Krienen, F.M., and Yeo, B.T.T. (2013). Opportunities and limitations of intrinsic functional connectivity MRI. *Nat. Neurosci.* 16, 832–837.
- Buzsáki, G. (2006). *Rhythms of the Brain*. (New York: Oxford University Press).
- Buzsáki, G., and Draguhn, A. (2004). Neuronal oscillations in cortical networks. *Science* 304, 1926–1929.
- Cochi, L., Zalesky, A., Fornito, A., and Mattingley, J.B. (2013). Dynamic cooperation and competition between brain systems during cognitive control. *Trends Cogn. Sci.* 17, 493–501.
- Cohen, A.L., Fair, D.A., Dosenbach, N.U.F., Miezin, F.M., Dierker, D., Van Essen, D.C., Schlaggar, B.L., and Petersen, S.E. (2008). Defining functional areas in individual human brains using resting functional connectivity MRI. *Neuroimage* 41, 45–57.
- Cole, M.W., Bagic, A., Kass, R., and Schneider, W. (2010). Prefrontal dynamics underlying rapid instructed task learning reverse with practice. *J. Neurosci.* 30, 14245–14254.
- Cole, M.W., Anticevic, A., Repovs, G., and Barch, D. (2011). Variable global dysconnectivity and individual differences in schizophrenia. *Biol. Psychiatry* 70, 43–50.
- Cole, M.W., Yarkoni, T., Repovs, G., Anticevic, A., and Braver, T.S. (2012). Global connectivity of prefrontal cortex predicts cognitive control and intelligence. *J. Neurosci.* 32, 8988–8999.
- Cole, M.W., Reynolds, J.R., Power, J.D., Repovs, G., Anticevic, A., and Braver, T.S. (2013). Multi-task connectivity reveals flexible hubs for adaptive task control. *Nat. Neurosci.* 16, 1348–1355.
- Cox, R.W. (1996). AFNI: software for analysis and visualization of functional magnetic resonance neuroimages. *Comput. Biomed. Res.* 29, 162–173.
- Doron, K.W., Bassett, D.S., and Gazzaniga, M.S. (2012). Dynamic network structure of interhemispheric coordination. *Proc. Natl. Acad. Sci. USA* 109, 18661–18668.
- Fair, D.A., Schlaggar, B.L., Cohen, A.L., Miezin, F.M., Dosenbach, N.U., Wenger, K.K., Fox, M.D., Snyder, A.Z., Raichle, M.E., and Petersen, S.E. (2007). A method for using blocked and event-related fMRI data to study "resting state" functional connectivity. *Neuroimage* 35, 396–405.
- Fischl, B. (2012). FreeSurfer. *Neuroimage* 62, 774–781.
- Fox, M.D., and Greicius, M. (2010). Clinical applications of resting state functional connectivity. *Front. Syst. Neurosci.* 4, 19.
- Fox, M.D., and Raichle, M.E. (2007). Spontaneous fluctuations in brain activity observed with functional magnetic resonance imaging. *Nat. Rev. Neurosci.* 8, 700–711.
- Fox, M.D., Snyder, A.Z., Vincent, J.L., and Raichle, M.E. (2007). Intrinsic fluctuations within cortical systems account for intertrial variability in human behavior. *Neuron* 56, 171–184.
- Fries, P. (2005). A mechanism for cognitive dynamics: neuronal communication through neuronal coherence. *Trends Cogn. Sci.* 9, 474–480.
- Friston, K.J. (1994). Functional and effective connectivity in neuroimaging: a synthesis. *Hum. Brain Mapp.* 2, 56–78.
- Friston, K.J. (2011). Functional and effective connectivity: a review. *Brain Connect.* 1, 13–36.
- Glasser, M.F., Sotiroopoulos, S.N., Wilson, J.A., Coalson, T.S., Fischl, B., Andersson, J.L., Xu, J., Jbabdi, S., Webster, M., Polimeni, J.R., et al.;

- WU-Minn HCP Consortium (2013). The minimal preprocessing pipelines for the Human Connectome Project. *Neuroimage* 80, 105–124.
- Goñi, J., van den Heuvel, M.P., Avena-Koenigsberger, A., Velez de Mendizabal, N., Betzel, R.F., Griffa, A., Hagmann, P., Corominas-Murtra, B., Thiran, J.-P., and Sporns, O. (2014). Resting-brain functional connectivity predicted by analytic measures of network communication. *Proc. Natl. Acad. Sci. USA* 111, 833–838.
- Greicius, M.D., Krasnow, B., Reiss, A.L., and Menon, V. (2003). Functional connectivity in the resting brain: a network analysis of the default mode hypothesis. *Proc. Natl. Acad. Sci. USA* 100, 253–258.
- Griswold, M.A., Jakob, P.M., Heidemann, R.M., Nittka, M., Jellus, V., Wang, J., Kiefer, B., and Haase, A. (2002). Generalized autocalibrating partially parallel acquisitions (GRAPPA). *Magn. Reson. Med.* 47, 1202–1210.
- Hasson, U., Nusbaum, H.C., and Small, S.L. (2009). Task-dependent organization of brain regions active during rest. *Proc. Natl. Acad. Sci. USA* 106, 10841–10846.
- Hebb, D.O. (1949). *The Organization of Behavior: A Neuropsychological Theory*. (Oxford: Wiley).
- Hermundstad, A.M., Bassett, D.S., Brown, K.S., Aminoff, E.M., Clewett, D., Freeman, S., Frithsen, A., Johnson, A., Tipper, C.M., Miller, M.B., et al. (2013). Structural foundations of resting-state and task-based functional connectivity in the human brain. *Proc. Natl. Acad. Sci. USA* 110, 6169–6174.
- Hutchison, R.M., Womelsdorf, T., Allen, E.A., Bandettini, P.A., Calhoun, V.D., Corbetta, M., Della Penna, S., Duyn, J.H., Glover, G.H., Gonzalez-Castillo, J., et al. (2013). Dynamic functional connectivity: promise, issues, and interpretations. *Neuroimage* 80, 360–378.
- Jutla, I.S., Jeub, L., and Mucha, P.J. (2011). A generalized Louvain method for community detection implemented in MATLAB. <http://netwiki.amath.unc.edu/GenLouvain>.
- Kelly, A.M.C., Uddin, L.Q., Biswal, B.B., Castellanos, F.X., and Milham, M.P. (2008). Competition between functional brain networks mediates behavioral variability. *Neuroimage* 39, 527–537.
- Kriegeskorte, N., Simmons, W.K., Bellgowan, P.S.F., and Baker, C.I. (2009). Circular analysis in systems neuroscience: the dangers of double dipping. *Nat. Neurosci.* 12, 535–540.
- Laird, A.R., Eickhoff, S.B., Rottschy, C., Bzdok, D., Ray, K.L., and Fox, P.T. (2013). Networks of task co-activations. *Neuroimage* 80, 505–514.
- Lancichinetti, A., and Fortunato, S. (2012). Consensus clustering in complex networks. *Sci. Rep.* 2, 336.
- Lewis, C.M., Baldassarre, A., Committeri, G., Romani, G.L., and Corbetta, M. (2009). Learning sculpts the spontaneous activity of the resting human brain. *Proc. Natl. Acad. Sci. USA* 106, 17558–17563.
- Mennes, M., Kelly, C., Colcombe, S., Castellanos, F.X., and Milham, M.P. (2013). The extrinsic and intrinsic functional architectures of the human brain are not equivalent. *Cereb. Cortex* 23, 223–229.
- Miller, E.K., and Cohen, J.D. (2001). An integrative theory of prefrontal cortex function. *Annu. Rev. Neurosci.* 24, 167–202.
- Mucha, P.J., Richardson, T., Macon, K., Porter, M.A., and Onnela, J.P. (2010). Community structure in time-dependent, multiscale, and multiplex networks. *Science* 328, 876–878.
- Power, J.D., Cohen, A.L., Nelson, S.M., Wig, G.S., Barnes, K.A., Church, J.A., Vogel, A.C., Laumann, T.O., Miezin, F.M., Schlaggar, B.L., and Petersen, S.E. (2011). Functional network organization of the human brain. *Neuron* 72, 665–678.
- Power, J.D., Mitra, A., Laumann, T.O., Snyder, A.Z., Schlaggar, B.L., and Petersen, S.E. (2014). Methods to detect, characterize, and remove motion artifact in resting state fMRI. *Neuroimage* 84, 320–341.
- Raichle, M.E. (2010). Two views of brain function. *Trends Cogn. Sci.* 14, 180–190.
- Raichle, M.E., MacLeod, A.M., Snyder, A.Z., Powers, W.J., Gusnard, D.A., and Shulman, G.L. (2001). A default mode of brain function. *Proc. Natl. Acad. Sci. USA* 98, 676–682.
- Rissman, J., Gazzaley, A., and D'Esposito, M. (2004). Measuring functional connectivity during distinct stages of a cognitive task. *Neuroimage* 23, 752–763.
- Ritchey, M., Yonelinas, A.P., and Ranganath, C. (2014). Functional connectivity relationships predict similarities in task activation and pattern information during associative memory encoding. *J. Cogn. Neurosci.* 26, 1085–1099.
- Sakai, K. (2008). Task set and prefrontal cortex. *Annu. Rev. Neurosci.* 39, 219–245.
- Smith, S.M., Fox, P.T., Miller, K.L., Glahn, D.C., Fox, P.M., Mackay, C.E., Filippini, N., Watkins, K.E., Toro, R., Laird, A.R., and Beckmann, C.F. (2009). Correspondence of the brain's functional architecture during activation and rest. *Proc. Natl. Acad. Sci. USA* 106, 13040–13045.
- Smith, S.M., Vidaurre, D., Beckmann, C.F., Glasser, M.F., Jenkinson, M., Miller, K.L., Nichols, T.E., Robinson, E.C., Salimi-Khorshidi, G., Woolrich, M.W., et al. (2013). Functional connectomics from resting-state fMRI. *Trends Cogn. Sci.* 17, 666–682.
- Traud, A.L., Kelsic, E.D., Mucha, P.J., and Porter, M.A. (2011). Comparing community structure to characteristics in online collegiate social networks. *SIAM Rev.* 53, 526–543.
- Ügurbil, K., Xu, J., Auerbach, E.J., Moeller, S., Vu, A.T., Duarte-Carvajalino, J.M., Lenglet, C., Wu, X., Schmitter, S., Van de Moortele, P.F., et al.; WU-Minn HCP Consortium (2013). Pushing spatial and temporal resolution for functional and diffusion MRI in the Human Connectome Project. *Neuroimage* 80, 80–104.
- van den Heuvel, M.P., Stam, C.J., Kahn, R.S., and Hulshoff Pol, H.E. (2009). Efficiency of functional brain networks and intellectual performance. *J. Neurosci.* 29, 7619–7624.
- Van Essen, D.C., Smith, S.M., Barch, D.M., Behrens, T.E.J., Yacoub, E., and Ugurbil, K.; WU-Minn HCP Consortium (2013). The WU-Minn Human Connectome Project: an overview. *Neuroimage* 80, 62–79.
- Vincent, J.L., Patel, G.H., Fox, M.D., Snyder, A.Z., Baker, J.T., Van Essen, D.C., Zempel, J.M., Snyder, L.H., Corbetta, M., and Raichle, M.E. (2007). Intrinsic functional architecture in the anaesthetized monkey brain. *Nature* 447, 83–86.
- Wig, G.S., Schlaggar, B.L., and Petersen, S.E. (2011). Concepts and principles in the analysis of brain networks. *Ann. N Y Acad. Sci.* 1224, 126–146.
- Yao, H., Shi, L., Han, F., Gao, H., and Dan, Y. (2007). Rapid learning in cortical coding of visual scenes. *Nat. Neurosci.* 10, 772–778.
- Zalesky, A., Fornito, A., and Bullmore, E. (2012). On the use of correlation as a measure of network connectivity. *Neuroimage* 60, 2096–2106.
- Zucker, R.S., and Regehr, W.G. (2002). Short-term synaptic plasticity. *Annu. Rev. Physiol.* 64, 355–405.